COMPARATIVE TESTS ON RESISTANCE TO CORROSION OF SOME NANOCOMPOSITES BASED ON TITANIUM-HYDROXYAPATITE

Dorinel TĂLPEANU[1], Anca COJOCARU[2], Raluca Ioana ZAMFIR (ANDRONIC)[3], Marin BANE[4], Sorin CIUCA[5*]

In this paper have been achieved some comparative tests regarding the resistance to corrosion of some nanocomposites materials based on Ti-HAp. The titanium and hydroxyapatite nanocomposite powder have been milled using a laboratory planetary mill with two work stations for 45h and then sintered at 900°C, 1000°C and 1075°C for 5 minutes by SPS process. The samples obtained have been characterized by X-ray diffraction (XRD) and by scanning electronic microscopy (SEM). The corrosion tests of Ti-HAp samples have been made by recording the evolution of open circuit potential in time followed by the potentiodynamic polarization.

Keywords: nanocomposites, titanium, hydroxyapatite, SPS, corrosion tests

1. Introduction

Nanocomposites of titanium hydroxyapatite (Ti-HAp) are considered to be of great interest in biomedical applications, especially in the implant due to the superior properties of the titanium and particular ability of hydroxyapatite ($Ca_{10}(PO_4)_6(OH)_2$) to form strong chemical bonds with bone tissue [1]. The titanium is the basic material most often used in implants due to its special characteristics as: high specific strength, high resistance to corrosion, great biocompatibility, complete inertia with the environment provided by the human body, increased capacity to adhere to tissues and bones [2, 3].

[1]Eng., National Institute for Research and Development in Electrical Engineering ICPE-CA, Romania, e-mail: dorinel.talpeanu@icpe-ca.ro
[2]Assoc. Prof., Dept. of Inorg. Chem., Phys. Chem. and Electrochem, University POLITEHNICA of Bucharest, Romania, e-mail: anca.cojocaru@chimie.upb.ro
[3]Prof., Dept.of Metallic Materials Science, Metal Materials Science Department, Metallurgy Physics, University POLITEHNICA of Bucharest, Romania, e-mail: ralucaza@yahoo.com
[4]Prof., Dept.of Metallic Materials Science, Physical Metallurgy, University POLITEHNICA of Bucharest, Romania, e-mail: marin.bane1@gmail.com
[5] Assoc. Prof., Dept.of Metallic Materials Science, Metal Materials Science Department, Metallurgy Physics, University POLITEHNICA of Bucharest, Romania
* Corresponding author, sorin.ciuca@upb.ro

High resistance to corrosion is a key feature in the longevity of a material used in implants. Natural titanium or titanium oxides anodically formed, that consist mainly of titanium dioxide (TiO_2), effectively protects the metal from its rapid dissolution in the harsh environments of the human body [4-6]. Also, the oxide film allows to the titanium to exhibit bioactivity in body fluids by providing a storage place of the calcium and phosphate compounds, thereby inducing ion exchange with apatite from the bone tissue [7]. Despite these bioactivities, the titanium does not promote the formation of mineral bone, which is necessary to fix rapidly the bone tissue of metal (osteo-integration). On the other hand, hydroxyapatite is often used in dental and orthopedic implants. However, its applications in the implants are limited due to its poor mechanical properties.

Hydroxyapatite has a good biocompatibility due to chemical and crystallographic structure similar to living bone tissue and a bioactivity due to partial resorption and replacement of natural bone shortly after implantation [1, 8, 9]. The nanocomposite made of Ti and HAp will have both the favorable properties of titanium and the bioactivity of hydroxyapatite. HAp bounded by titanium is an alternative to increase the bioactivity to the implant surface. However, current techniques have major issues related to the interface bounding between metal and ceramic material [10]. Low adhesion of the ceramic material to metal often causes the exfoliation of the ceramic coating, which leads to failure of the implant.

Hydroxyapatite, due to its chemical and crystallographic structure similar to that of the mineral bone tissue, seems to be best suited for implants. However, due to poor mechanical properties of hydroxyapatite, it is not suited to portable applications [11].

On the other hand, titanium and titanium alloys are mainly used in biomedical applications due to their superior properties such as low coefficient of elasticity, good resistance to fatigue and resistance to corrosion. Low coefficient of elasticity of titanium and titanium alloys is widely seen as a bio-mechanical advantage because it can result from a low stress shielding. The low density of titanium alloys provides a specific strength-to-weight ratio that allows weaker and stronger structures.

Titanium and titanium alloys exhibit relatively weak tribological properties due to its weak hardness [12]. Nevertheless, titanium and its alloys are generally considered to have a good biocompatibility and a high resistance to corrosion [7, 8].

Excellent biocompatibility of the hydroxyapatite and good mechanical properties of the titanium make this nanocomposite a promising candidate in the development of medical applications. There are two methods to establish a connection between those two materials: the first method is the manufacturing of a

composite by using powder of titanium and hydroxyapatite [9-13], and the second method is to change the titanium surface using hydroxyapatite as coating [14,15].

Due to the great differences between physical and thermal properties between titanium and hydroxyapatite, the first method appears to be more effective [16]. Following the studies, a significant effect of energy absorption mechanism due to plastic deformation of flexible titanium particles from the cracks has been found in the Ti-HAp microcrystalline composites [17].

Excellent biocompatibility of the hydroxyapatite with good mechanical properties of titanium make this nanocomposite a promising candidate in the development of medical applications.

The corrosion resistance is an important property for materials used as implants. Titanium and its alloys have been used extensively in biomedical applications due to their good resistance to corrosion and high biocompatibility [18-24]. These alloys show good corrosion resistance thanks to protective films, especially TiO_2 [25-30]. Composite materials studied in this paper are made from titanium and hydroxyapatite with different production parameters. It is necessary to characterize the corrosion behavior of materials in oral fluids.

The aim of this study is to investigate the composition and some obtain parameters effect to corrosion behavior of composite materials based on titanium and hydroxyapatite in oral fluids.

In this paper are presented the results obtain from elaboration of Ti-HAp nanocomposites with 2%HAp, by SPS technique, at different sintering parameters 900-1075˚C and their compositional and structural characterization by XRD and SEM and evaluation corrosion resistance.

2. Experimental

Materials and methods

2.1. Preparation of Ti-HAp nanocomposites

For achieving nanocomposite Ti-HAp were used ceramic nanopowders by hydroxyapatite, prepared by precipitation from aqueous solutions, and titanium powder, 99.4% purity, provenance of Merck.

For the preparation of nanopowders of hydroxyapatite have been used as starting materials: calcium nitrate ($Ca(NO_3)_24H_2O$) and ammonium hydrogen phosphate ($(NH_4)_2HPO_4$), both of analytical purity (Merck provenance). To adjust the pH of the solution was used 25% NH_3 (NH_4OH), analytical purity (Fluka provenance). They were selected raw materials of high purity with high solubility in water. The dosage of the raw materials was performed HAp corresponding to the stoichiometry of the compound for which the ration Ca/Pr = 1.67.

The starting materials were dosed analytical balance after which they were dissolved in distilled water to 2000 ml glasses, to give concentration 0.5 M solutions. Blending the two different solutions was performed using a mechanical

stirrer at a speed in the range of 350-380 rev/min for 1 h, a solution of ammonium phosphate is introduced dropwise into the calcium ion-containing solution. Maintaining a constant pH (pH = 8-9) and the mixture solution was homogenized for a further 2 hours. The precipitate obtained was filtered with filter paper by using of the vacuum pump (about 45 min), washed with distilled water, after which it was dried in an oven at 80°C for 24 hours. the dried material was milled and calcined at 900°C for 2 hours.

Obtaining the nanocomposite powder was performed by mechanical milling by using a laboratory planetary mill with two work stations (model Retsch PM 400). The amount of the hydroxyapatite powder added in relation to the milling of titanium powder is 2%. For milling in two powders under optimal conditions were used stainless steel balls, and the ratio of the powders and balls was 1:10 and the speed of 200 rpm for 45h.

Nanocomposites powder was sintered by using the installation by spark plasma sintering (FCT Systeme GmbH, type D 25 HP). The milled sample was introduced into high-density graphite mold having an inside diameter of 20 mm, between the graphite sheet and wrapped in felt. Prepared mold was placed inside the plant. Achieving the samples using sintering machine in the plasma spark was carried out in a vacuum, the pressure force of 16 kN. The heating rate was 50°C/min, the temperature of sintering used was 900°C, 1000°C and 1075^{o}C, with plateau five minutes at maximum temperature. After completion of sintering, cooling samples was achieved rapidly with a velocity of 50^{o}C/min.

Table 1

Codification of samples and processing parameters to SPS

Current number	Sample code	HAp percent [%]	Method of production	Temperatura [^{o}C]	Force [kN]
1.	P1	2	SPS	900	16
2.	P2	2	SPS	1000	16
3.	P3	2	SPS	1075	16

2.2. X-ray diffraction

The X-ray diffraction (XRD) pattern of the sample is excited with a monochromatic radiation of known wavelength, to measure the interplanar spacing of the Bragg equation.

For the analysis of crystallographic phases measurements were carried out in Bragg Brentano geometry, using a Bruker D8 Discover diffractometer model with Cu radiation, equipped with LynxEye detector 1D. Crystallographic phases identification was performed by using 2014 Release ICDD database.

2.3. Scanning Electron Microscopy

For the microstructural characterization was used scanning electron microscopy (SEM), which was highlighted both the morphological appearance of

the microstructure obtained materials and distribution of qualitative and quantitative evaluation phase granular porosity structural material. Analysis by electron microscopy sintered materials was performed by using a scanning electron microscope FESEM-FIB Auriga.

2.4. Electrochemical corrosion studies

The corrosion behavior of the composite Ti-HAp samples was investigated by recording the evolution of open circuit potential in time followed by the potentiodynamic polarization.

The electrochemical measurements were carried out using a three electrode thermostated cell with the composite sample as working electrode (S=2.3 cm^2), the reference electrode was a Radiometer Analytical saturated silver/silver chloride electrode immersed directly into the solution, and a platinum grid was the counter electrode.

Prior to each experiment, the electrode surface was polished with emery paper, rinsed with disilled water and dried.

The electrochemical measurements were carried out using a Voltalab 40, Radiometer Analytical potentiostat/galvanostat interfaced with a computer using VoltaMaster 4.0 software for data acquisition and data processing. The test solutions were thermostated during all the experiments at 37±1^oC.

Polarization curve measurements were obtained at a scan rate of 2 mV/sec starting from cathodic to anodic direction in the potential range -500 to +500mV versus free potential.

Electrochemical impedance spectroscopy (EIS) was carried out at the open-circuit potentials in the frequency range 100 kHz- 100 mHz with a sinusoidal potential perturbation of 10mV amplitude.

The open-circuit potential (OCP) versus time and potentiodynamic polarization curves were recorded. Corrosion potential (E_{corr}) and corrosion current density (i_{corr}) were determined from polarization curves by the Tafel extrapolation method.

Electrochemical tests were carried out in aerated solution of Fusayama-Mayer artificial saliva prepared using analytical grade reagents and double distilled water (Table 2).

Table 2

The composition of the Fusayama-Mayer artificial saliva used for electrochemical studies [31]

Compound	Concentration
NaCl	0.4
KCl	0.4
$CaCl_2$ $2H_2O$	0.906
NaH_2PO_4 $2H_2O$	0.690
Na_2S $9H_2O$	0.005
Urea $CO(NH_2)_2$	1

The corrosion parameters: corrosion potential (E_{corr}), corrosion current density (i_{corr}) and polarization resistance (R_p) obtained from the potentiodynamic polarization curves were used to evaluate the corrosion resistance of Ti-HAp composite materials. Before the potentiodynamic polarizations tests the samples were left under an open circuit condition in the solution for 30 minutes to attend a stable value of the potential.

3. Results and discussions

3.1. The compositional and structural characterization

In Fig. 1 shows the diffraction nanocomposite titanium and hydroxyapatite after a preliminary milling for 45h and then obtained after process by spark plasma sintering (SPS) at 1000^{o}C. Following the sintering process, there was no evidence crystallographic phase side, which is due to both the quality of raw materials (analytical purity) used and the degree of compactness level obtained from processing through in plasma spark sintering. Fig. graph of diffraction X shows the presence of two phases in the material Ti and HAp processed by SPS at 1000^{o}C for 5 min.

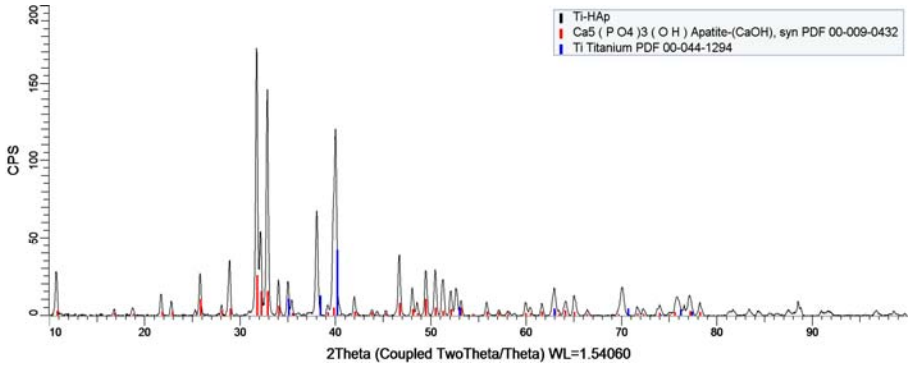

Fig. 1. X-ray diffractogram of sample of the SPS Ti HAp sintered at 1000 ^{o}C for 5 minutes

In Fig. 2 shows the microstructure of nanocomposite microcrystalline that highlights the existence of a microporosity inherent in sintered materials. However the pores are very small have a spherical shape which indicates that the sintering parameters have been correctly selected. Surface morphology reveals cleavage phenomena attributed to mechanical stresses induced by mechanical milling.

a). 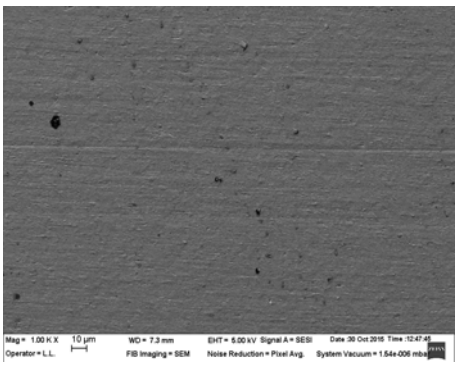 b). 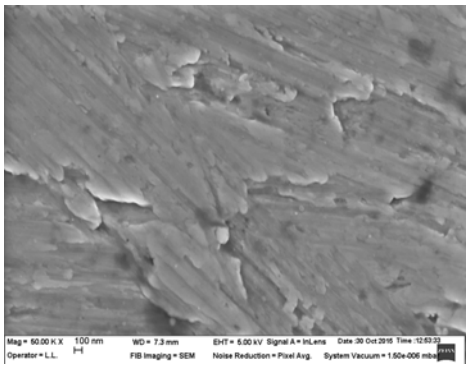

Fig. 2. Electron Microscopy sample obtained from SPS (1075 oC) morphostructurally general aspect (secondary electrons) (a), morphostructurally aspect in detail (secondary electrons) (b)

3.2. Eltrochemical analysis

The open circuit potential of the samples was measured for 30 minutes in Fusayama-Mayer artificial saliva. The results are shown in Fig. 4 tested samples. All the curves demonstrated similar trends of a plain variation of potential with immersion time at a value close to 0 V. The curves show an oscilation of potential probably indicating an active-passive behavior due to a local oxidation.

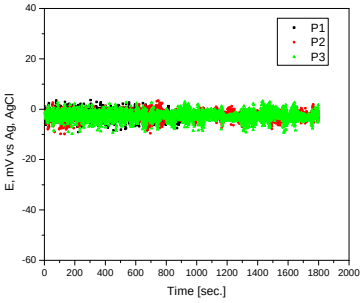

Fig. 4. Open circuit potential versus time curves samples P1, P2 and P3 in Fusayama-Mayer artificial saliva at 37±1°C

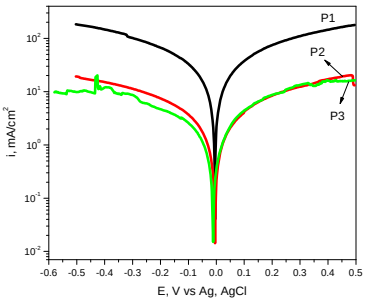

Fig. 5. Potentiodynamic polarization for samples P1, P2 and P3 in Fusayama-Mayer artificial saliva at 37±1°C

The potentiodynamic polarization results for samples P1, P2 and P3 in Fusayama-Mayer artificial saliva at 37±1°C are presented in Fig. 5. All curves show a similar behavior for the tested samples. Both cathodic and anodic curves have the same aspect due to the same anodic and cathodic processes occurring of the surface of each of the studied samples not influenced by the sintering temperature of the samples.

Electrochemical parameters obtained from the polarization curves are listed in Table 3. These include the corrosion potential (E_{corr}) and the corrosion current density (i_{corr}), both determined by extrapolation of the Tafel lines, as well as anodic Tafel slope (b_a) and cathodic Tafel slope for hydrogen evolution (b_c).

Table 3

Corrosion parameters calculated from the potentiodynamic polarization curves (Tafel) for P1, P2 and P3 in usayama-Mayer artificial saliva at 37±1°C

Sample	E_{corr}, mV vs.Ag, AgCl	Rp, Ω cm^2	i_{corr}, mA/cm^2	b_a, mV/dec	-b_c, mV/dec
P1	-10	2.80	2.1905	36	39
P2	-9	25.97	0.2209	35	36
P3	-16	33.06	0.1735	29	37

As can be seen from Table 3 the best corrosion resistance was obtained for sample P3. The corrosion current density is 0.1735 mA/cm^2 for P3, more than one order of magnitude lower than that obtained for sample P1, and the polarization resistance is 33.06 Ω cm^2.

The results show that the increase of the sintering temperature gives a higher corrosion resistance for the Ti-HAp composite.

Table 4

Electrochemical parameters obtained from the processing of electrochemical impedance spectroscopy results for samples P1, P2 and P3

Sample		Solution resistance, R_s, Ω·cm^2	Polarization Resistance, R_p, Ω·cm^2	Double layer capacitance, C_{dl} mF/cm^2
P1	Before	2.453	0.1314	4.265
	After	2.880	0.0081	88.26
P2	Before	9,41	0.2687	0.5922
	After	4.86	0.0547	29.09
P3	Before	30.21	4.35	1.157
	After	27.90	11.19	0.319

The increase polarization resistance 11.19 Ω·cm^2 (4.35 Ω·cm^2 measured before corrosion) and double layer capacity reduction after corrosion (0.319 mF/cm^2 beside 1.157 mF/cm^2) for P3 sample indicate the increased resistance for the sample in oral fluids beside P1 and P2 samples. The results of electrochemical impedance spectroscopy confirm the results of potentiodynamic polarization.

4. Conclusions

The nanocomposite powder obtain by mechanical milling process for 45h, was sintered by SPS technique, and we obtain samples with ø = 20mm and h = 3mm. The samples were sintered at different temperatures (900°C, 1000°C and

1075°C), power press 50MPa, heating / cooling speed 50°C/min and time of exposure 10 min.

The samples obtain by SPS were then characterized by X-ray diffraction, structural characterization by SEM and corrosion test were made in oral fluids Fusayama-Mayer type that was prepared by using p.a. substances and distilled water.

Comparing the corrosion behavior of titanium-hydroxyapatite samples obtained after spark plasma sintering (at 900°C, 1000°C and 1075°C) in oral fluids it has been found that the sample sintered at the highest temperature (1075°C) has Rp polarization resistance after the corrosion higher than the sample sintered at 900°C thereby increasing the sintering temperature improve the corrosion resistance of the sample.

R E F E R E N C E S

[1]. *P. Laffargue, H. J. Breme, J. A. Helsen, H. F. Hildebrand*, Metals as biomaterials, in: J. A. Helsen, H. J. Breme (eds.), John Wiley and Sons, Chichester, 1998;

[2]. *L. Wang, Y. Liu, Z. Zhang (eds.)*, Handbook of nanophase and nanostructured materials, Z Kluwer Academic / Plenum Publishers, New York, vol. 1–4, 2003;

[3]. *G.J. Peelen, B. V. Rejda and K. De Groot*, Preparation and Properties of Sintered Hydroxyapatite, vol. 74, pp. 1487-1510, 1991;

[4]. *C. Suryanarayna*, Mechanical alloying and milling, Progr. Mater. Sci., vol.46, pp. 101-141, 2001;

[5]. *M. Jurczyk*, The progress of nanocrystalline hydride electrode materials, Bulletin of the polish academy of sciences technical sciences, vol. 52, pp. 67-77, 2004;

[6]. *E. S. Thian, N. H. Loh, K. A. Khor, S. B. Tor*, Microstructures and mechanical properties of powder injection molded Ti-6Al-4V/HA powder, Biomaterials, vol. 23, pp. 2927–2938, 2002;

[7]. *X. Liu, P. K. Chu, Ch. Ding*, Titanium-Hydroxyapatite Nanocomposites, Mater. Sci. Eng., vol. 47, pp. 229-239, 2004;

[8]. *A Zhecheva, W Sha, S Malinov*, A Long, Enhancing the microstructure and properties of titanium alloys through nitriding and other surface engineering methods, Surface and Coatings Technology, vol. 200, pp. 2192-2207, 2005;

[9] *Craciunescu, Oana; Moldovan, Lucia; Tardei, Christu; et al.*, Carbodiimide Cross-Linked Nanocomposite Materials Designed for Bone Tissue Regeneration, MATERIALE PLASTICE, Volume: 47, Issue: 1, Pages: 59-63, Published: MAR 2010

[10]. *H. Ji, C. B. Ponton, P. M. Marquis*, Microstructural Characterization of Hydroxyapatite Coating on Titanium, J. Mater. Sci.: Mater. Med., vol. 3, pp. 283-287, 1992;

[11]. *L.L. Hench*, Bioceramics: Materials and Applications, J. Am. Ceram. Soc., vol. 81, pp. 1705–1728, 1998;

[12].*C. Chenglin, Z. Jingchuan, Y. Zhongda, W. Shidong*, Hydroxyapatite-Ti functionally graded biomaterial fabricated by powder metallurgy, Mater.Sci. Eng., vol. 271, pp. 95-100, 1999;

[13]. *S. A. Pepargyri, D. Tsipas, G. Stergioudis, J. Chlopek*, Eng. Biomater., 46, 27, 2005;

[14]. *A. Bibi, E. Boanini, B. Bracci, A. Facchini, S. Panzavolta, F. Segati, L. Sturla*, Biomaterials, 26, 4085, 2005;

[15]. *W. P. Cao, L. L. Hench*, Biomaterials, Ceramics International, vol. 22, pp. 493-507, 1996;

[16]. *C. Chu, X. Xue, J. Zhu, Z. Yin*, Fabrication and characterization of ... hydroxyapatite for use as heavy load-bearing hard tissue replacement, J. Mater. Sci. Mater. Med., vol. 17, pp. 245–25, 2006;

[17]. *C. Chu, P. Lin, Z. Dong, X. Xiu, J. Yhu, Z. Yin, J.* Mater. Sci.: Mater. Med., vol. 13, pp. 985-990, 2002;

[18]. *J.C.M. Souza, S.L. Barbosa, E. Ariza, J.-P. Celis, L.A. Rocha*, Simultaneous degradation by corrosion and wear of titanium in artificial saliva containing fluorides, Wear 292–293 (2012), pp. 82–88;
[19]. *K. Indira, U. Kamachi Mudali, N. Rajendran*, Corrosion behavior of electrochemically assembled nanoporous titania for biomedical applications, Ceramics International 39 (2013), pp. 959-967;
[20]. *Lidia Benea, Eliza Danaila, Pierre Ponthiaux*, Effect of titania anodic formation and hydroxyapatite electrodeposition on electrochemical behaviour of Ti–6Al–4V alloy under fretting conditions for biomedical applications, Corrosion Science 91 (2015), pp. 262-271;
[21]. *Yong Huang, Shuguang Han, Xiaofeng Pang, Qionqion Ding, Yajing Yan*, Electrodeposition of porous hydroxyapatite/calcium silicate composite coating on titanium for Biomedical applications, Applied Surface Science 271 (2013), pp. 299-302;
[22]. *Duraisamy Ramesh, Thiagarajan Vasudevan*, Evaluation of Corrosion Stability of Water Soluble Epoxy-Ester Primer through Electrochemical Studies, Materials Sciences and Applications, 2012, 3, pp. 333-347;
[23]. *Ilven Mutlu, Enver Oktay*, Characterization of 17-4 PH stainless steel foam for biomedical applications in simulated body fluid and artificial saliva environments, Materials Science and Engineering C 33 (2013) 1125–1131;
[24]. *Yong Huang, Yajing Yan, Xiaofeng Pang*, Electrolytic deposition of fluorine-doped hydroxyapatite/ZrO2 films on titanium for biomedical applications, Ceramics International 39 (2013) 245–253;
[25]. *Irma C. Matos, Ivan N. Bastos, Marília G. Diniz, and Mauro S. de Miranda*, Corrosion in artificial saliva of a Ni-Cr-based dental alloy joined by TIG welding and conventional brazing, The Journal of Prosthetic Dentistry, 114(2), 2015, pp. 278-285;
[26]. *A. Vladescu, M. Braic, F. Ak Azem, I. Titorencu, V. Braic, V. Pruna, A. Kiss, A. C. Pararu, I. Birlik*, Applied Surface science 354 (2015), pp. 373-379;
[27]. *Delphine Veys-Renaux, Zouhir Ait El Haj, Emmanuel Rocca*, Corrosion resistance in artificial saliva of titanium anodized by plasma electrolytic oxidation in Na_3PO_4, Surface & Coatings Technology 285 (2016), pp. 214-219;
[28]. *Lv Jinlonga, Liang Tongxiang*, Improved corrosion resistance of 316L stainless steel by nanocrystalline and electrochemical nitridation in artificial saliva solution, Applied Surface Science 359 (2015) 158–165;
[29]. *Chao Zhang, Jiming Liu, Wenwen Yu, Daqian Sun, Xinhua Sun*, Susceptibility to corrosion of laser welding composite arch wire in artificial saliva of salivary amylase and pancreatic amylase, Materials Science and Engineering C 55 (2015) 267–271;
[30]. *Irma C. Matos, Ivan N. Bastos, Marília G. Diniz, and Mauro S. de Miranda*, Corrosion in artificial saliva of a Ni-Cr-based dental alloy joined by TIG welding and conventional brazing, The Journal of Prosthetic Dentistry, 114(2), 2015, pp. 278-285;
[31]. *Chao Zhang, Jiming Liu, Wenwen Yu, Daqian Sun, Xinhua Sun*, Susceptibility to corrosion of laser welding composite arch wire in artificial saliva of salivary amylase and pancreatic amylase, Materials Science and Engineering C 55 (2015) 267–271.